Available online at www.sciencedirect.com
ScienceDirect
Food Chemistry 110 (2008) 590–597
FOOD CHEMISTRY
www.elsevier.com/locate/foodchem

Effects of selenium supplementation on rat heart apex and right ventricle myocardia by using FTIR spectroscopy: A cluster analysis and neural network approach

Neslihan Toyran [a,*], Feride Severcan [b], Mete Severcan [c], Belma Turan [d]

[a] Department of Physiology, Faculty of Medicine, Baskent University, 06530 Ankara, Turkey
[b] Department of Biological Sciences, Middle East Technical University, 06531 Ankara, Turkey
[c] Electrical and Electronics Engineering Department, Middle East Technical University, 06531 Ankara, Turkey
[d] Department of Biophysics, School of Medicine, Ankara University, 06100 Ankara, Turkey

Received 29 November 2007; received in revised form 1 February 2008; accepted 14 February 2008

Abstract

The effects of selenium supplementation on apex and right ventricle myocardia of the rat heart were investigated using Fourier transform infrared (FTIR) spectroscopy by examining the changes in the frequency values of major absorptions arising from lipids and proteins. Cluster analysis was used to discriminate the selenium treated group from the control by utilizing two distinct spectral regions, belonging to absorptions arising from lipids and proteins, respectively. In addition, protein secondary structures were predicted using neural network analysis. The results suggest that selenium treatment at a non-toxic dose causes some significant structural alterations in lipids and proteins of rat heart apex and right ventricle myocardia, which might be revealing a slight deleterious effect of selenium supplementation.

Keywords: Selenium; Myocardium; FTIR spectroscopy; Cluster analysis; Neural networks; Protein secondary structure estimation

1. Introduction

Selenium (Se) is an essential nutrient of great importance to human health due to its antioxidant effect. Se deficiency has been linked to the development of many health problems, including heart diseases. In recent years, interest concerning Se has increased remarkably due to its effect in human, either as a toxic or an essential element depending on its concentration. Plant foods, meats and see foods are the major dietary sources of Se. The content of Se in food depends mainly on the Se content of the soil where the plants are cultivated or where the animals are raised. The recommended dietary allowances were established as 70 μg Se/day for a healthy adult man and 55 μg Se/day for a healthy adult woman by the Food and Nutrition Board of the United States Research Council (Navarro-Alarcon & Lopez-Martinez, 2000). Se present in most vegetables is in highly available form, which is around 85–100%. Despite the usually highest Se content in seafood, available Se ranges from 20% to 50%, being usually less than 25%. Meat products have a Se bioavailability of approximately 15% (Navarro-Alarcon, de la Serrana, Perez-Valero, & Lopez-Martinez, 1998). Dairy products have the lowest bioavailability ranging from less than 2% in ewe milk to 7% in cow and goat milk (Shen, Van Dael, & Deelstra, 1993). Direct sign for the essential needs of Se in human nutrition was not found until 1979, when a research group discovered relationships between the low concentrations of Se in a geographical area named Keshan in China and an endemic congestive cardiomyopathy called

* Corresponding author. Tel.: +90 312 2341010x1567; fax: +90 312 2341180.
E-mail address: toyran@baskent.edu.tr (N. Toyran).

0308-8146/$ - see front matter © 2008 Elsevier Ltd. All rights reserved.
doi:10.1016/j.foodchem.2008.02.044

"Keshan disease". Recently, the scientific concern of Se has increased as a result of several studies performed, since it seems that low Se levels could be another factor in the origin of some other human diseases, such as cancer and diabetes in addition to cardiovascular diseases (Bergqvist, Chee, Lutchka, Rychik, & Stallings, 2003; Navarro-Alarcon, Lopez-G. de la Serrana, Perez-Valero, & Lopez-Martinez, 1999; Ozgen et al., 2007). In general, tissues having high metabolic activity such as liver, and heart also have high vulnerability to oxidative stress (Navarro-Alarcon & Lopez-Martinez, 2000). The beneficial effects of Se consumption at adequate levels can be due to its role in the antioxidant enzymes, and its effects on fat metabolism (Navarro-Alarcon & Lopez-Martinez, 2000). Nyyssonen, Porkkala, Salonen, Korpela, and Salonen (1994) established that Se has a protective effect against oxidation of serum LDL- and VLDL-cholesterol in a double-blind clinical trial.

In one of our previous studies, Se (5 μmol/kg/day for four weeks)-induced changes in the concentrations of several macromolecules such as lipids, proteins, and glycogen were determined by analysing only the intensity values of various absorptions in Fourier transform infrared (FTIR) spectra belonging to the left and the right ventricle myocardia, and small veins of the normal rat heart (Toyran, Turan, & Severcan, 2007). The effects of Se on the macromolecular structures of heart tissues are unknown yet. Therefore, the aim of the present study was to investigate the effects of Se supplementation on protein and lipid structure of rat apex and right ventricle myocardia by using FTIR microspectroscopy, which is a combination of IR spectroscopy and microscopy. Furthermore, in the current study, cluster analysis was applied on FTIR spectra which permitted a rapid and reliable differentiation between the control and Se treated samples, in both lipid (2800–3050 cm^{-1}) and protein (1480–1800 cm^{-1}) regions based on the spectral variations between these two groups. We have chosen to study these specific regions of the heart due to their clinical importance in terms of both diagnosis and treatment of heart diseases (Manolis, 2006).

The protein region was investigated by neural network analysis, utilizing the amide I band (1600–1700 cm^{-1}) of FTIR spectra to estimate Se-induced changes in the protein secondary structure of apex and right ventricle myocardia. In the last 10 years, the application of artificial neural networks has become an efficient tool for structure identification based on data obtained by FTIR spectroscopy (Akkas, Severcan, Yilmaz, & Severcan, 2007; Severcan, Haris, & Severcan, 2004). Major advantage of FTIR spectroscopy technique over conventional ones is that many statistical and multivariate approaches can be performed to analyse the data for spectrally biodiagnosing the tissues. This novel spectroscopic method visualizes the underlying chemistry of the tissue, based on hundreds of vibrational absorption bands arising from the samples (Boskey & Camacho, 2007; LeVine & Wetzel, 1994).

2. Materials and methods

2.1. Sample preparation and data acquisition

Experimental animals belonging to the control and Se treated groups were prepared as described previously (Toyran et al., 2007). Weanling Wistar rats (Ankara University, Faculty of Medicine, Animal Care Facility) were maintained at an ambient air temperature of $22 \pm 1\ ^{\circ}C$ and a 12 h light/dark cycle. The rats were fed with standard rat nutrient and water without restriction. All the procedures used in the experiments were approved by the Ethics Committee of Ankara University, Faculty of Medicine. The rats were categorized into two groups as (1) Control group, and (2) Se treated group. The rats belonging to the control group were injected with 0.1 M citrate buffer (pH 4.5) intraperitoneally (i.p.) as a single dose and fed without any restriction. The rats belonging to the Se treated group were injected with 5 μmol/kg/day sodium selenite i.p. for four weeks. Then, the animals were sacrificed under anesthesia by opening their chest (pentobarbital, 30 mg/kg). For acquisition of spectral data, two serial cross-sections having 9 μm thicknesses were obtained from the apex and right ventricle myocardia of all groups. These sections were thaw-mounted on IR-transparent CaF_2 windows for spectral measurements. A small amount of optimum cutting tool was applied to tissue samples to attach the sections to the cryotome. For all samples, the first sections taken from all tissues were used for FTIR microspectroscopy measurements and the second serial sections were used for Hematoxylin & Eosin (H&E) staining to see the histologically defined tissue regions. FTIR microspectroscopic mapping was done on all the rat heart tissues. An IR microscope (Bruker, Germany) coupled with FTIR spectrometer (Bruker, Germany) was used to map the tissue sections as described previously (Toyran et al., 2007). Spectra were collected in both x and y directions in steps of 80 μm for the apex, and in steps of 56 μm for the right ventricle myocardium to obtain IR data completely covering the chosen tissue areas. IR spectra were collected in absorption from 850 to 4000 cm^{-1}. The spectral resolution was set to 6 cm^{-1}. For apex, 64 scans; for right ventricle myocardium, 256 scans were co-added per pixel spectrum. To get rid of spectral contributions from water vapor and CO_2, the spectrometer was continuously purged with dry air.

2.2. Spectral analysis

CytoSpec and OPUS data collection software packages were used for spectral analysis. The "quality test" of the raw spectral data was the first step of the data evaluation procedure. Quality tests were carried out as described previously (Toyran, Lasch, Naumann, Turan, & Severcan, 2006). The spectra which have passed the quality test were used for first derivative calculations in 950–1480 and 2800–3050 cm^{-1} spectral regions. A five smoothing point

Savitzky–Golay algorithm was used while performing first derivative calculations. Then the vector-normalization was done using the first derivatives in the frequency range of 950–1480 cm^{-1}. First derivative spectra were used for cluster analyses, which were performed in 950–1480 and 2800–3050 cm^{-1} regions to identify tissue structures with CytoSpec program for apex. Image assembly on the basis of cluster analysis is based on the idea of assigning a distinct colour to all spectra in one cluster. In this way, It was possible to obtain the average spectra arising from the myocardium of the rat apex. The original absorption spectra and their averages belonging to different clusters were saved. Then, for further spectral analysis, the data were loaded into OPUS. For right ventricle myocardium, cluster analysis was not performed for structural identification, because there was no other tissue structure on the spectrally mapped region of the rat hearts to be distinguished.

2.3. Cluster analysis

For comparison of normal and Se treated cardiac apex and right ventricle myocardia, cluster analyses were performed on second derivative spectra using a nine smoothing point Savitzky–Golay algorithm in 2800–3050 cm^{-1} and 1480–1800 cm^{-1} spectral regions for the analysis of signals arising from lipids and proteins, respectively. Spectral distances were calculated between pairs of spectra as Pearson's correlation coefficients, as described by Helm, Labischinski, Schallehn, and Naumann (1991). Cluster analysis for separation of the control and Se treated groups was based on Euclidean distances. Ward's algorithm provided by the OPUS software was used for hierarchical clustering. Cluster analysis examines the interpoint distances between all the samples and represents the information in the form of dendogram, which is a two dimensional plot. In a dendogram, the cluster of samples was formed based on their closeness in row space. Cluster analysis is a kind of multivariate statistical analysis procedure which can be considered as an objective method, meaning that no trained spectroscopist is needed to evaluate the experimental results and differentiate between the control and Se treated groups.

2.4. Neural network analysis

Neural network models have been generated to predict protein secondary structure contents from the FTIR spectra using Neural Networks Toolbox of MATLAB. We used a data set containing FTIR spectra of 18 water soluble proteins whose secondary structure contents are known from X-ray crystallography (Lee, Haris, Chapman, & Mitchell, 1990). To improve the prediction accuracy, the size of the data set was increased by interpolating the available FTIR spectra. Before training the neural networks, the FTIR spectra were normalized and their discrete cosine transforms were obtained. Discrete cosine transform compacts the significant information in each spectrum in low frequency coefficients of the transform which are used as inputs to the neural networks (Jain, 1986). Bayesian regulation was used to train the neural networks whose structures were optimized in terms of the number of inputs, number of hidden units and the threshold for sum squared errors. The trained neural networks have standard error of prediction values of 4.19% for α-helix, 3.49% for β-sheet. The details of the training and testing algorithm can be found in Severcan et al. (2004).

2.5. Statistical analysis

The results were displayed as "mean ± standard error of mean". To test the significance of the differences between the control and Se treated group, Mann–Whitney U test was performed. Values of p less than 0.05 were accepted as significantly different from the control group. The degree of significance was demonstrated as $^{*}p < 0.05$, $^{**}p < 0.01$.

3. Results

The current study was designed to investigate the effects of Se supplementation for four weeks on protein and lipid structures of rat cardiac apex and right ventricle myocardia by monitoring the changes in the wavenumber values of main absorptions arising from lipids and proteins. In addition, cluster analysis was used to differentiate between Se treated and control groups. The regions used for cluster analysis are shown in Fig. 1. Finally, Se-induced changes in the protein secondary structure were estimated by using neural networks based on amide I band.

Fig. 2a shows the H&E staining image of a section having 9 μm thickness taken from the rat heart apex at 25× magnification and the mapped region on this section is shown in square on the same figure. After FTIR microscopy measurements, the data were loaded to CytoSpec program for data analysis. The image of cluster analysis, which was performed to discriminate the signals arising from myocardium of the apex from the rest of the tissue, is shown in Fig. 2b. In this figure, it is possible to see three different clusters given with different colours belonging to different components of the tissue. The original average absorption spectra of these clusters were recorded separately. The light gray colour arises from the tissue freezing medium (optimum cutting tool), the white colour arises from the epicardium of the apex and the tissue freezing medium. The cluster represented by gray colour belongs to the myocardium of the apex. The spectra tested for poor quality were excluded from all consecutive evaluations and are shown with black colour in the figure. The purpose of this cluster analysis was to obtain the average original absorption spectra arising from the myocardium of the apex since we are interested in the changes occurring only in this particular region of the heart between control and Se treated groups. For comparisons, the data belonging to this cluster representing the myocardium was used.

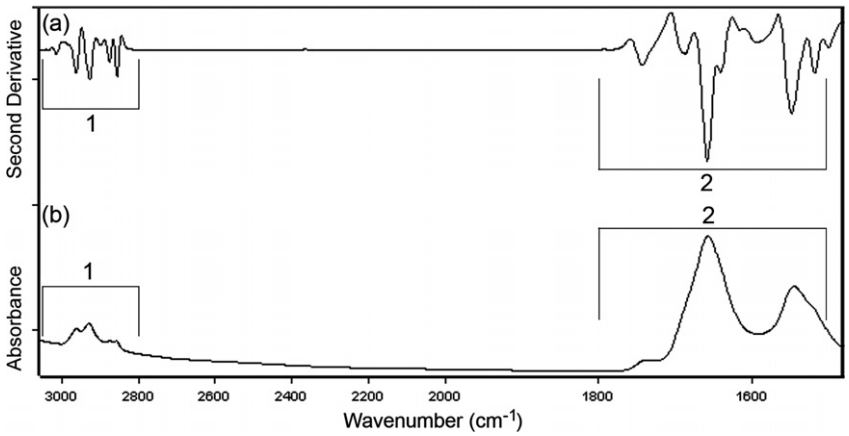

Fig. 1. Representative spectra. Second derivative (a) and absorption (b) spectra of the control apex myocardium. The signals mainly originating from lipids in 2800–3050 cm^{-1} spectral region are shown with "1"; and the signals mainly originating from proteins in 1480–1800 cm^{-1} spectral region are shown with "2" in the figure.

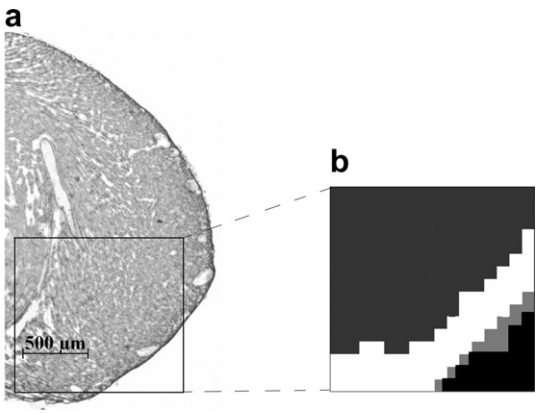

Fig. 2. Light microscope images and mapped regions of the rat heart. H&E staining image of a section having 9 µm thickness taken from the rat heart apex at 25× magnification (a), and the mapped region on this section is shown in square. The image of cluster analysis (b).

The cluster analysis was performed for the apex part of all the rat hearts and the original average spectrum arising from myocardium was saved in a format readable by OPUS. Then all the data were loaded into OPUS program for further analysis.

Changes in the wavenumber values of the main absorptions in apex and right ventricle myocardia of the control and the Se treated groups are shown in Table 1. As clearly seen in the table, Se treatment led to slight but significant shifts in the wavenumber of CH_2 asymmetric (2926 cm^{-1}) and symmetric stretching (2855 cm^{-1}) vibrations to lower values from 2926.48 ± 0.10 to $2925.83^{*} \pm 0.09$ and from 2855.24 ± 0.14 to $2854.77^{*} \pm 0.04$, respectively, for apex myocardium. Parallel but more significant Se-induced changes were observed for the right ventricle myocardium. As seen in Table 1, the wavenumber of amide I band (1655 cm^{-1}) also shifts to lower values from 1654.86 ± 0.09 to $1654.18^{*} \pm 0.04$ for the apex myocardium and from 1654.78 ± 0.10 to $1654.14^{**} \pm 0.06$ for the right ventricle myocardium. The next step was performing cluster analysis for comparison of normal and Se treated groups for both apex and right ventricle myocardia of the rat heart. The results of cluster analysis using 2800–3050 and 1480–1800 cm^{-1} spectral regions of normal and Se treated groups for apex and right ventricle myocardia are shown in Figs. 3 and 4, respectively. Hierarchy of clusters from individual elements is represented as dendograms, which are tree-like diagrams showing the arrangements of the clusters. As seen from the Figs. 3 and 4, two distinct clusters were produced corresponding to control and Se treated groups for both apex and right ventricle myocardia in the spectral regions subjected to

Table 1
The wavenumber values of the Infrared bands for control and Se treated groups of apex and right ventricle myocardia

Functional groups	Apex myocardia		Right ventricle myocardia	
	Control ($n = 6$)	Selenium ($n = 4$)	Control ($n = 8$)	Selenium ($n = 4$)
CH_3 asym str. (2958)	2958.90 ± 0.09	2958.81 ± 0.11	2959.01 ± 0.03	2958.89 ± 0.08
CH_2 asym str. (2926)	2926.48 ± 0.10	$2925.83^{*} \pm 0.09$	2926.56 ± 0.03	$2925.96^{**} \pm 0.07$
CH_3 sym str. (2873)	2872.90 ± 0.03	2872.82 ± 0.07	2872.93 ± 0.03	2872.92 ± 0.02
CH_2 sym str. (2855)	2855.24 ± 0.14	$2854.77^{*} \pm 0.04$	2855.14 ± 0.03	$2854.74^{**} \pm 0.06$
Amide I (1655)	1654.86 ± 0.09	$1654.18^{*} \pm 0.04$	1654.78 ± 0.10	$1654.14^{**} \pm 0.06$
Amide II (1542)	1542.42 ± 0.20	1542.34 ± 0.23	1542.68 ± 0.08	1542.46 ± 0.24

Data shown as "mean ± standard error of mean". $p < 0.05$ were accepted as significantly different from the control group. The degree of significance was denoted as $^{*}p < 0.05$, $^{**}p < 0.01$.

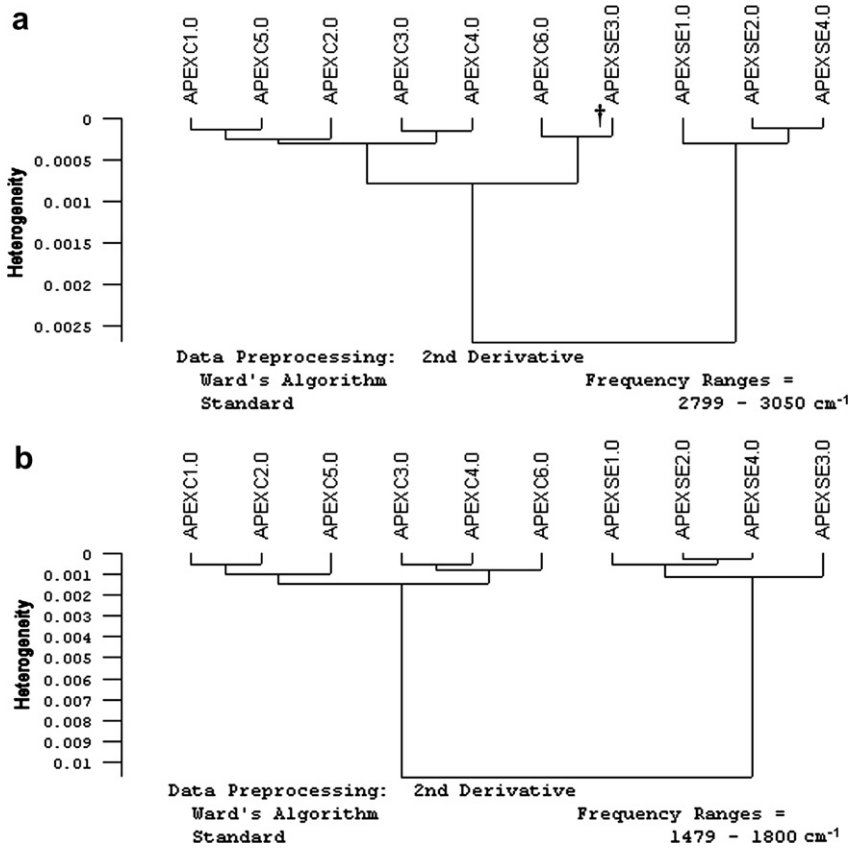

Fig. 3. Cluster analysis results of apex myocardium. Results of cluster analysis belonging to the apex myocardium in 2800–3050 cm^{-1} spectral region (a), and in 1480–1800 cm^{-1} spectral region (b). Ward's algorithm was used for hierarchical clustering. Cluster analyses was performed on second derivative spectra using a nine smoothing point Savitzky–Golay algorithm. APEXC1.0 refers to Apex myocardium of the control group, first sample, and so on; APEXSE1.0 refers to Apex myocardium of Se treated group, first sample, and so on.

cluster analysis. There occurred only one misclassification (Se treated group as control) which is shown with "†" in Fig. 3a; and two misclassifications (Se treated group as control) in 2800 and 3050 cm^{-1} spectral region which are shown with "†" in Fig. 4a.

The protein region, corresponding to absorption values between 1600 and 1700 cm^{-1} was further analysed using neural networks based on FTIR data to estimate the Se-induced alterations on protein secondary structure. The results are presented in Table 2. It is clearly seen from the table that Se supplementation caused slight changes in the protein secondary structure of cardiac apex myocardium by decreasing the content of α-helix and by increasing the content of β-sheet structures. Similar but statistically significant changes occurred in the protein secondary structure profile of the right ventricle myocardium due to Se treatment ($p < 0.05$).

4. Discussion

Increased oxidative stress is known to be involved in the pathogenesis of chronic heart failure. Functioning as an antioxidant, Se is definitely important for the prevention and treatment of chronic heart failure (de Lorgeril & Salen, 2006). Consequently, the use of Se supplements has been very popular by healthy individuals in order to be protected from oxidative stress-related diseases such as cardiovascular diseases, diabetes, and cancer. On the other hand, some type of intoxication can appear when daily dietary Se intake exceed the capacity of the human body to eliminate it. So, it is crucial to understand the exact molecular mechanism of its effects. Morphological and molecular changes occurring especially in the cardiac apex and right ventricle myocardia are very important for the maintenance and regulation of the normal electrical activity of the heart (Winfield, Graham, Benghuzzi, Tucci, & Cameron, 2003). In the present study, 5 μmol/kg/day of Se, which is known to be a non-toxic dose, is given to the rats for four weeks to see its effects at molecular level by using FTIR spectra.

The 2800–3050 cm^{-1} region is dominated by C–H stretching vibrations of the fatty acyl chains of membrane lipids, and the spectral region dominated by protein bands lies between 1800 and 1400 cm^{-1} (Cakmak, Togan, & Severcan, 2006). Shifts in wavenumber values of the IR bands are used to obtain valuable structural information about the investigated tissue (Cakmak et al., 2006). The frequencies of the CH_2 stretching bands of the acyl chains depend on the degree of conformational order/disorder state of lip-

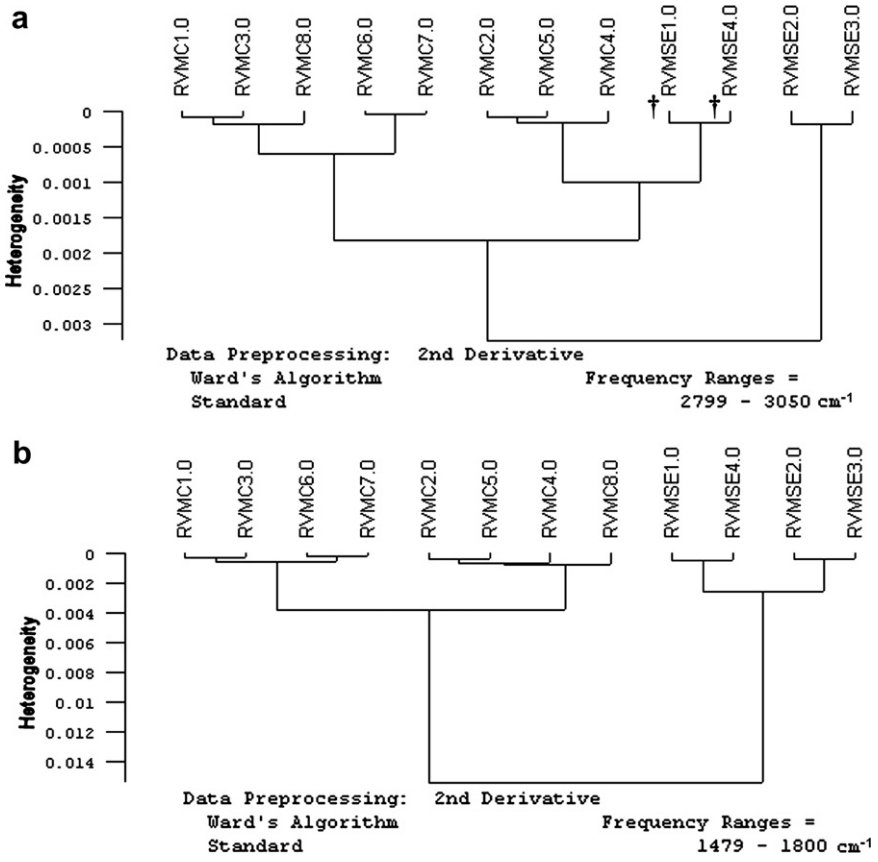

Fig. 4. Cluster analysis results of right ventricle myocardium. Results of cluster analysis belonging to the right ventricle myocardium in 2800–3050 cm^{-1} spectral region (a), and in 1480–1800 cm^{-1} spectral region (b). Ward's algorithm was used for hierarchical clustering. Cluster analyses was performed on second derivative spectra using a nine smoothing point Savitzky–Golay algorithm. RVMC1.0 refers to right ventricle myocardium of the control group, first sample, and so on. RVMSE1.0 refers to right ventricle myocardium of Se treated group, first sample, and so on.

Table 2
The results of neural network predictions based on FTIR data in 1600–1700 cm^{-1} spectral region for the changes in protein secondary structure between control and Selenium treated groups

Functional groups	Apex myocardia		Right ventricle myocardia	
	Control ($n = 6$)	Selenium ($n = 4$)	Control ($n = 8$)	Selenium ($n = 4$)
α-Helix	69.88 ± 2.34	63.33 ± 8.35	71.75 ± 1.90	50.70^{**} ± 3.70
β-Sheet	11.70 ± 2.83	22.9 ± 15.64	11.86 ± 2.69	32.52^{*} ± 7.66

Data shown as "mean ± standard error of mean". $p < 0.05$ were accepted as significantly different from the control group. The degree of significance was denoted as: $^{*}p < 0.05$, $^{**}p < 0.01$.

ids (lipid acyl chain flexibility) (Kazanci, Toyran, Haris, & Severcan, 2001; Toyran & Severcan, 2002). For example, lower frequency implies lower acyl chain flexibility (ordering). In the present study, the CH_2 asymmetric stretching band around 2925 cm^{-1} and the symmetric CH_2 stretching band around 2855 cm^{-1} shifted slightly but significantly to lower values in Se treated groups of apex and right ventricle myocardia (Table 1), meaning that lipid order increases and acyl chain flexibility decreases. The results of the current study suggested for the first time that Se induces an increase in the state-of-order of lipids of the apex and right ventricle myocardia. We have previously reported significant increases in the intensities of the CH_2 symmetric and asymmetric stretching bands in the left and the right ventricle myocardia, and small veins of the rat heart due to Se treatment (Toyran et al., 2007). These reported increases in the content of the CH_2 groups might be a possible explanation for the Se-induced increase in the order of lipids observed in the present study. It is known that the content of CH_2 bands may increase in the case of an increase in the acyl chain length of phospholipids. A well known property of a membrane is that, an increase in the chain length will end up with an increase in the lipid main phase transition temperature and the thickness of the bilayer, which will lead to a more stable lipid structure. The increase we have observed in the lipid order parameter can be very important in the context of its effect on membrane function. The change in the order of lipids may even effect the membrane potential

and permeability by altering ion channel kinetics (Szalontai, Nishiyama, Gombos, & Murata, 2000).

The band located around 1655 cm^{-1} can be attributed to amide I, and located around 1542 cm^{-1} can be attributed to amide II vibrations of structural proteins (Haris & Severcan, 1999). Since the positions of amide bands are sensitive to protein conformation, the changes in the wavenumber values of these bands were analysed. The observed shift in the wavenumber value of the amide I band to lower values upon Se treatment in both apex and right ventricle myocardia might be indication of some important structural alterations in the existing proteins and/or the expression of new types of proteins. To achieve a more detailed analysis, we used neural networks based on FTIR spectroscopy. The estimation of secondary structure of proteins is a crucial first step in understanding how the amino acid sequence of a protein determines the native state (Chandonia & Karplus, 1999). FTIR spectroscopy enabled us to monitor Se-induced structural alterations rapidly and sensitively in proteins in untreated, unstained and unfixed whole tissue samples without destroying the native structure of the proteins. In recent years, neural networks have seen to be a reliable method used for the prediction of protein secondary structure contents (Bohm, 1996). The results of neural network analysis of the current study suggest that 5 μmol/kg/day of Se supplementation causes alterations in the protein secondary structure by decreasing the α-helix and increasing the β-sheet contents, more dramatically in the right ventricle myocardium (Table 2). The changes observed in the structure of cardiac tissue proteins might be due to altered redox potential which can affect cell function by modifying the protein structure, even in the absence of apparent deleterious changes in the heart function (Ayaz, Ozdemir, Yaras, Vassort, & Turan, 2005). Se-induced structural changes occurring in the proteins may possibly alter the phospholipids' behavior such as the changes in the order of membrane lipids. The order of membrane lipids might have increased in the present study to compensate the Se-induced changes in the protein structure (Zehmer & Hazel, 2004).

We successfully differentiated between the Se treated and control groups for both apex and right ventricle myocardia using cluster analysis in order to obtain objective classification solely on the basis of spectral patterns. This analysis clearly separated control and Se treated groups (Figs. 3 and 4). These findings reveal that Se treatment causes some important changes in the FTIR spectra in both lipid and protein regions, which can successfully be determined by applying cluster analysis.

The findings of the current study mainly reveal that Se treatment causes important changes in FTIR spectra in both lipids and proteins of the heart, and changes the protein profile in favour of β-sheet structure, significantly in the right ventricle myocardium. Certain human diseases, which are generally called conformational diseases, are associated with proteins that misfold and exhibit decreased solubility under physiological conditions. Furthermore, dysfunctional aggregations of proteins in non-native conformations occur (Nandi, 1996). Neurodegenerative diseases are the most commonly known examples of these diseases. In these disease states, there is a change in secondary structure of proteins from native α-helix to filamentous aggregate forming β-sheet structures (Ronga et al., 2007). Similar situation was also observed in diabetes (Toyran et al., 2006). The increase we have observed in the order of lipids together with the alterations in the secondary structure of proteins mentioned above may have great importance in the regulation of membrane functions of cardiac tissue. All these structural changes might be a pointing out a slight deleterious effect of Se supplementation. Consequently, extra precaution is needed in using Se supplements by healthy individuals due to its possible pro-oxidant effect in addition to its reported beneficial effects. These findings have provided significant insight on the effect of Se treatment on normal apex and right ventricle myocardia of the rat heart. The effect of Se in the cardiovascular diseases should be considered in future long term studies concomitantly with other nutrients involved in the oxidative stress such as vitamins E and C, β-carotene and phenolic compounds. Therefore future trials of supplementation should be focused on the concomitant administration and study of these supplements in order to have a better knowledge of their resulting effect in different diseases.

Acknowledgment

This work was supported by Baskent University research fund: DA07/39.

References

Akkas, S. B., Severcan, M., Yilmaz, O., & Severcan, F. (2007). Effects of lipoic acid supplementation on rat brain tissue: An FTIR spectroscopic and neural network study. *Food Chemistry, 105*, 1281–1288.

Ayaz, M., Ozdemir, S., Yaras, N., Vassort, G., & Turan, B. (2005). Selenium-induced alterations in ionic currents of rat cardiomyocytes. *Biochemical Biophysical Research Communication, 327*, 163–173.

Bergqvist, A. G., Chee, C. M., Lutchka, L., Rychik, J., & Stallings, V. A. (2003). Selenium deficiency associated with cardiomyopathy: A complication of the ketogenic diet. *Epilepsia, 44*, 618–620.

Bohm, G. (1996). New approaches in molecular structure prediction. *Biophysical Chemistry, 59*, 1–32.

Boskey, A., & Camacho, N. P. (2007). FT-IR imaging of native and tissue-engineered bone and cartilage. *Biomaterials, 28*, 2465–2478.

Cakmak, G., Togan, I., & Severcan, F. (2006). 17Beta-estradiol induced compositional, structural and functional changes in rainbow trout liver, revealed by FT-IR spectroscopy: A comparative study with nonylphenol. *Aquatic Toxicology, 77*, 53–63.

Chandonia, J. M., & Karplus, M. (1999). New methods for accurate prediction of protein secondary structure. *Proteins, 35*, 293–306.

de Lorgeril, M., & Salen, P. (2006). Selenium and antioxidant defenses as major mediators in the development of chronic heart failure. *Heart Failure Reviews, 11*, 13–17.

Haris, P. I., & Severcan, F. (1999). FTIR spectroscopic characterization of protein structure in aqueous and non-aqueous media. *Journal of Molecular Catalysis B: Enzymatic, 7*, 207–221.

Helm, D., Labischinski, H., Schallehn, G., & Naumann, D. (1991). Classification and identification of bacteria by Fourier-transform infrared spectroscopy. *Journal of General Microbiology, 137*, 69–79.

Jain, A. K. (1986). *Fundamentals of digital image processing*. Englewood Cliffs, NJ: Prentice Hall.

Kazanci, N., Toyran, N., Haris, P. I., & Severcan, F. (2001). Vitamin D_2 at high and low concentrations exert opposing effects on molecular order and dynamics of dipalmitoyl phosphatidylcholine membranes. *Spectroscopy – An International Journal, 15*, 47–55.

Lee, D. C., Haris, P. I., Chapman, D., & Mitchell, C. R. (1990). Determination of protein secondary structure using factor-analysis of infrared spectra. *Biochemistry, 29*, 9185–9193.

LeVine, S. M., & Wetzel, D. (1994). In situ chemical analyses from frozen tissue sections by Fourier transform infrared microspectroscopy. Examination of white matter exposed to extravasated blood in the rat brain. *American Journal of Pathology, 145*, 1041–1047.

Manolis, A. S. (2006). The deleterious consequences of right ventricular apical pacing: Time to seek alternate site pacing. *Pacing and Clinical Electrophysiology, 29*, 298–315.

Nandi, P. K. (1996). Protein conformation and disease. *Veterinary Research, 27*, 373–382.

Navarro-Alarcon, M., de la Serrana, H. L., Perez-Valero, V., & Lopez-Martinez, C. (1998). Serum selenium levels as indicators of body status in cancer patients and their relationship with other nutritional and biochemical markers. *Science of the Total Environment, 212*, 195–202.

Navarro-Alarcon, M., Lopez-G de la Serrana, H., Perez-Valero, V., & Lopez-Martinez, C. (1999). Serum and urine selenium concentrations as indicators of body status in patients with diabetes mellitus. *Science of the Total Environment, 228*, 79–85.

Navarro-Alarcon, M., & Lopez-Martinez, M. C. (2000). Essentiality of selenium in the human body: Relationship with different diseases. *Science of the Total Environment, 249*, 347–371.

Nyyssonen, K., Porkkala, E., Salonen, R., Korpela, H., & Salonen, J. T. (1994). Increase in oxidation resistance of atherogenic serum lipoproteins following antioxidant supplementation: A randomized double-blind placebo-controlled clinical trial. *European Journal of Clinical Nutrition, 48*, 633–642.

Ozgen, I. T., Dagdemir, A., Elli, M., Saraymen, R., Pinarli, F. G., Fisgin, T., et al. (2007). Hair selenium status in children with leukemia and lymphoma. *Journal of Pediatric Hematology Oncology, 29*, 519–522.

Ronga, L., Palladino, P., Costantini, S., Facchiano, A., Ruvo, M., Benedetti, E., et al. (2007). Conformational diseases and structure-toxicity relationships: Lessons from prion-derived peptides. *Current Protein & Peptide Science, 8*, 83–90.

Severcan, M., Haris, P. I., & Severcan, F. (2004). Using artificially generated spectral data to improve protein secondary structure prediction from Fourier transform infrared spectra of proteins. *Analytical Biochemistry, 332*, 238–244.

Shen, L., Van Dael, P., & Deelstra, H. (1993). Evaluation of an in vitro method for the estimation of the selenium availability from cow's milk. *Zeitschrift fur Lebensmittel Untersuchung und Forschung, 197*, 342–345.

Szalontai, B., Nishiyama, Y., Gombos, Z., & Murata, N. (2000). Membrane dynamics as seen by fourier transform infrared spectroscopy in a cyanobacterium, Synechocystis PCC 6803. The effects of lipid unsaturation and the protein-to-lipid ratio. *Biochimica et Biophysica Acta, 1509*, 409–419.

Toyran, N., Lasch, P., Naumann, D., Turan, B., & Severcan, F. (2006). Early alterations in myocardia and vessels of the diabetic rat heart: an FTIR microspectroscopic study. *Biochemical Journal, 397*, 427–436.

Toyran, N., & Severcan, F. (2002). Infrared spectroscopic studies on the dipalmitoyl phosphatidylcholine bilayer interactions with calcium phosphate: Effect of vitamin D_2. *Spectroscopy – An International Journal, 16*, 399–408.

Toyran, N., Turan, B., & Severcan, F. (2007). Selenium alters the lipid content and protein profile of rat heart: An FTIR microspectroscopic study. *Archives of Biochemistry and Biophysics, 458*, 184–193.

Winfield, A. K., Graham, J. T., Benghuzzi, H., Tucci, M., & Cameron, J. (2003). The role of sustained delivery of corticosterone alone or in combination with antioxidants on the cardiovascular system of adult female rats. *Biomedical Science Instruments, 39*, 353–358.

Zehmer, J. K., & Hazel, J. R. (2004). Membrane order conservation in raft and non-raft regions of hepatocyte plasma membranes from thermally acclimated rainbow trout. *Biochimica et Biophysica Acta – Biomembranes, 1664*, 108–116.